Cancer Research

Microenvironment and Immunology

Inherent and Tumor-Driven Immune Tolerance in the Prostate Microenvironment Impairs Natural Killer Cell Antitumor Activity

Christine Pasero[1,2], Gwenaëlle Gravis[2], Mathilde Guerin[2], Samuel Granjeaud[1], Jeanne Thomassin-Piana[2], Palma Rocchi[1,2], Maria Paciencia-Gros[2], Flora Poizat[2], Mélanie Bentobji[2], Francine Azario-Cheillan[2], Jochen Walz[2], Naji Salem[2], Serge Brunelle[2], Alessandro Moretta[3], and Daniel Olive[1,2,4]

Abstract

The field of immunotherapy for solid tumors, such as prostate cancer, has been recently focusing on therapies that can counter tumor-mediated immunosuppression. Precise quantification and characterization of the immune infiltrates in tumors is crucial to improve treatment efficacy. Natural killer (NK) cells, major components of the antitumor immune system, have never been isolated from prostate tumors, despite their suspected role in disease progression. Here, we examined the frequency, phenotype, and functions of NK cells infiltrating control and tumor prostate tissues. NK cell infiltrates in prostate tissues were mainly CD56 (NCAM1)-positive and displayed an unexpected immature, but activated, phenotype with low or no cytotoxic potential. Furthermore, we show that TGFβ1 (TGFB1) is highly secreted into the prostate environment and partly mediates the immunosuppressive effects on NK cells. In addition to this basal level of immunotolerance to NK cells, the prostate environment became further resistant to NK cell–mediated immunity upon cancer cell infiltration. Coculture experiments revealed that prostate cancer cells induced the expression of inhibitory receptor (ILT2/LILRB1) and downregulated the expression of activating receptors NKp46 (NCR1), NKG2D (KLRK1), and CD16 (FCGR3) by NK cells, thus preventing their recognition of tumor cells. Notably, blood levels of NKp46 were also decreased in prostate cancer patients and were inversely correlated with levels of prostate-specific antigen, the main prognostic factor in prostate cancer. Our study shows that a strong immunosuppressive environment impairs NK cell function at multiple levels in prostate cancer and provides a rationale for the design of therapies that restore NK cell efficiency in the prostate tumor microenvironment. *Cancer Res; 76(8); 2153–65. ©2016 AACR.*

Introduction

Prostate cancer is one of the most frequent causes of cancer mortality among men (1) and is still incurable once it becomes metastatic. Androgen-deprivation therapy (ADT) is the mainstay of treatment for advanced prostate cancer, but resistance to castration inevitably develops. Immunotherapy has been introduced as an alternative therapeutic approach with Sipuleucel-T and GVAX-PCa cell-based cancer vaccines, or Ipilimumab (anti-CTLA-4) mAb (2). Over the past few years, the immune infiltrate and its prognostic significance have attracted a lot of attention (3); however, infiltrating lymphocytes are poorly characterized in prostate. Thus, the interaction between immune system and cancer cells within the patient's tumor needs to be better understood in order to develop clinically effective immunotherapies.

Natural killer (NK) cells are innate cytotoxic lymphocytes that play a fundamental role in antitumor immunity (4). Mice lacking NK cells or defective for NK cell receptors have a higher incidence of spontaneous tumors (5). A 11-year follow-up study reported that a low degree of NK cell cytotoxicity was correlated with increased cancer risk in men (6). NK cells can be broadly divided in CD56^{dim} cytotoxic subset, which represent the majority of NK cells in the blood, and in CD56^{bright} cytokine producer subset (7). The activation of NK cells is regulated by a balance between activating and inhibitory signals transmitted through surface receptors that determine the cytotoxic response (8). Inhibitory receptors include the killer immunoglobulin-like receptors (KIR), CD94/NKG2A, and ILT2/CD85j. The main activating receptors of NK cells are the natural cytotoxicity receptors (NCRs: NKp46, NKp30, NKp44), NKG2D and DNAM-1 (DNAX accessory molecule-1).

Tumor cells have developed several mechanisms to evade from NK immunosurveillance, through the modulation of cell surface molecules or the release of immunosuppressive soluble factors such as PGE2 or TGFβ1 in the tumor microenvironment (9, 10). Alterations of NCRs have been observed in blood from acute myeloid leukemia patients (11), and recent studies show that intratumoral NK cells display phenotypic and/or functional alterations compared with peripheral NK cells in breast cancer (12, 13), lung cancer (14–16), colorectal cancer (17), renal cell

[1]Centre de Recherche en Cancérologie de Marseille, INSERM U1068/CNRS U7258, Marseille, France. [2]Institut Paoli-Calmettes, Marseille, France. [3]D.I.M.E.S., University di Genova, Genova, Italy. [4]Aix Marseille Université, Marseille, France.

Note: Supplementary data for this article are available at Cancer Research Online (http://cancerres.aacrjournals.org/).

Corresponding Authors: Daniel Olive, Institut Paoli Calmettes Inserm U1068, 232 bd Sainte Marguerite, Marseille 13009, France. Phone: 334-8697-7271; Fax: 334-9122-3610; E-mail: daniel.olive@inserm.fr; and Christine Pasero, christine.pasero@inserm.fr

doi: 10.1158/0008-5472.CAN-15-1965

©2016 American Association for Cancer Research.

AACR

carcinoma (18), and gastrointestinal stromal tumors (GIST; refs.19, 20).

In prostate cancer, the ligands for NKp30 and NKp46 were found to be expressed on primary tumors but not on benign prostate hyperplasia (21). Importantly, increased NK cell infiltrate within prostate tumors was found to be associated with a lower risk of progression through IHC, providing evidence that NK cells may have a protective role against prostate cancer in humans (22). However, prostate-infiltrating NK cells have never been isolated and their phenotype and functions remain unknown. Indeed, the isolation of tumor-infiltrating immune components is problematic due to the small size of prostate samples and the infiltrative growth of the tumor within the gland.

We, therefore, set out to analyze and compare for the first time NK cell phenotype and functions in tumor but also control prostate tissues, in comparison with NK cells isolated from peripheral blood of prostate cancer patients (pB-PC). Our results reveal two unexpected levels of tissue tolerance to NK cells in prostate cancer; first, NK cells infiltrating the prostate gland display immature phenotype with hyporesponsive functional status; second, the tumor breaks the balance between activating and inhibitory NK cell receptors. Together, these alterations lead to a profound immunosuppressive environment that should be targeted to restore NK cell cytotoxicity against prostate cancer.

Patients and Methods

Patients
Prostate cancer patients were prospectively recruited in a comprehensive cancer center (Institut Paoli-Calmettes IPC, Marseille, France) and provided written informed consent. The project was reviewed by the internal review board and the study was approved by a central national ethics committee.

Tumor tissues were obtained from 21 prostate cancer patients (mean age 71.9 years) including $n = 16$ localized (Loc) or locoregional (LCR) tumors and $n = 5$ metastatic (M) tumors. Clinical characteristics of the tumors can be found as Supplementary Table S1. The mean follow-up period was 12.1 months. Control prostate tissues ($n = 20$, mean age 66.9 years) were collected from prostate cancer patients, in an area selected out of the tumor site by pathologists, or from bladder cancer patients at the time of cystoprostatectomy. All sections were strictly selected by a single pathologist (J. Thomassin-Piana). Blood samples (pB-PC) were obtained from 18 patients with localized prostate cancer (mean age 61 years) and from 30 patients with metastatic prostate cancer (mean age 65 years). Blood samples from healthy men volunteers (mean age 51 years) were used as controls (Etablissement Français du Sang (EFS, Marseille, France).

Isolation of lymphocytes from blood
Peripheral blood mononuclear cells (PBMC) were purified from blood samples by Lymphoprep (lymphocyte separation medium) density gradient centrifugation. PBMCs were washed and resuspended in RPMI (Gibco, Life Technologies) medium for further analysis.

Isolation of lymphocytes from prostate tissues
Fresh prostate tissues were extemporaneously treated and mechanically minced using scalpels in RPMI medium. Cell suspensions obtained were filtered successively through 70- and 30-μm cell strainers (Miltenyi Biotec). The supernatant was harvested and centrifuged at high speed to remove residual cellular ele-

ments. This supernatant, referred as "dissociation supernatant" was aliquoted and frozen at $-20°C$ until further use in functional experiments. Cell suspension was washed and used directly for flow cytometry staining.

Cell lines
PC3 cell line is derived from a late-stage castrate-resistant metastatic prostate cancer sample and was purchased from ATCC. PC3 was cultured in DMEM (Gibco Life Technologies) supplemented with 10% fetal calf serum (FCS, Lonza). K562 cell line is derived from human erythroleukemia cell line (ATCC) and was cultured in RPMI supplemented with 10% FCS.

Flow cytometry
Cells were incubated with conjugated antibodies or isotypic controls (listed in Supplementary Table S2) for 30 minutes at 4°C, washed and extemporaneously collected on a BD LSR Fortessa cytometer (BD Biosciences), and analyzed with FACSDiva (BD Biosciences) or FlowJo (TreeStar Inc.) softwares. For NK cells, the gating strategy consisted on the elimination of the doublets based on FSC-A/FSC-H parameters, followed by the removal of dead cells using a cell viability marker. NK cell population was defined as $CD3^-CD56^+$ cells within the lymphocyte gate. The phenotypic data in the article are represented as percentage of cells positive for a given marker (bimodal expression); or the mean ratio fluorescence intensity (RMFI, unimodal expression), that is, the ratio between the mean fluorescence intensity (MFI) of cells stained with the selected mAb and that of cells stained with isotypic control alone.

CD107 degranulation and IFNγ/TNFα production
PBMCs were activated overnight in IL2 (100 UI/mL; Chiron) and IL15 (10 ng/mL; Miltenyi Biotec), and incubated with K562 target cells at effector: target (E:T) ratio of 10:1 during 4 hours, with monensin (Golgi Stop), FITC-conjugated anti-CD107a (LAMP1), and FITC-conjugated anti-CD107b (LAMP2) mAbs (BD Biosciences). Then PBMCs were stained for 30 minutes at 4°C with PerCP-Cy5.5–conjugated anti-CD3 and PC7-conjugated anti-CD56 antibodies and permeabilized with Cytofix/Cytoperm (BD Biosciences). Intracellular antibodies were next added (IFNγ and TNFα) before cell analysis.

^{51}Cr experiments
Blocking mAbs directed against NK cell receptors or related ligands were produced in A. Moretta's laboratory: anti-NKp30 (F252), anti-NKp46 (KL247), anti-2B4 (CO54), anti-DNAM (F5), anti-NKG2D (ON72). Purified NK cells from healthy donors or patients were incubated at various effector: target (E:T) ratios (10:1, 5:1, 2:1) in triplicate, with ^{51}Cr-labeled K562–positive control cell line, in the presence of blocking mAbs or saturating concentrations of appropriate isotype controls. Four hours later, supernatants were harvested and assayed for the release of ^{51}Cr. Spontaneous and total lysis were measured by incubating target cells in the absence of NK cells and in the presence of NP40, respectively. The percentage of specific lysis was measured as follows: (experimental lysis – spontaneous lysis)/(maximum lysis-spontaneous lysis) $\times$ 100.

Detection of soluble factors and cytokines
sMICA, ADAM17, TGFβ1, and PGE2 secretion were evaluated by ELISA (R&D Systems). IL1ra, MCP-1, RANTES, and IL8 secretion were evaluated in a 9-plex multiple human cytokine assay

(Bio-Plex; Bio-Rad). IL1β, IL4, IL6, IFNγ, and TNFα were not detected in the supernatants. This assay was run according to the manufacturer's recommended procedure; beads were read on the Bio-Plex suspension array system and data were analyzed using Bio-Plex manager software with 5PL curve fitting.

IHC

Immunohistochemical staining was performed on 3-μm thick sections of formalin-fixed paraffin-embedded prostate tissues fixed in 4% formol alcohol. Slides were incubated for 20 minutes in a 98°C water bath (pH 9 for both NKp46 and CD3). After neutralization of the endogenous peroxidase (EnVision FLEX Peroxidase blocking reagent; Dako) and saturation, sections were layered with the anti-NKp46 polyclonal antibody (R&D Systems, 1/40e) or the anti-CD3 polyclonal antibody (Dako, FLEX Ready-to-use). The primary antibody was incubated for 6 hours (anti-NKp46 antibody) or 20 minutes (anti-CD3 antibody). Sections were revealed with the EnVision FLEX/HRP Kit (Dako), DAB substrate Kit (Dako), counterstained with the EnVision FLEX hematoxylin substrate buffer (Dako), and mounted using Pertex (Histolab). Controls were performed by incubating slides with second antbody alone.

Statistical analyses

All statistical analyses were performed using GraphPad Prism software (GraphPad). The nonparametric tests (paired Wilcoxon test or unpaired Mann–Whitney test) are indicated in the figure legends. Only P values inferior to 0.05 were considered as significant. Heatmaps were performed using multi-experiment viewer of the TM4 micro-array software suite (TMeV); version 4.9 was retrieved from http://www.tm4.org/mev.html.

Results

NK cells infiltrating the prostate gland display peculiar phenotype and low cytotoxic potential

We first investigated NK cell infiltration on paraffin-embedded prostate tissues by immunohistochemical staining using the NK cell–specific marker NKp46 (Fig. 1A). The results show that prostate tissues are poorly infiltrated by NK cells, in comparison with T cells that were detected with anti-CD3 antibody (Fig. 1B). Both populations were mainly localized in the stroma surrounding normal and tumor prostatic glands. We prospectively collected tumor ($n = 21$) and control prostate tissues ($n = 20$) to investigate infiltrating NK cell phenotype, by comparison with NK cells isolated from peripheral blood of prostate cancer patients (pB-PC, $n = 10$). Lymphocytes were isolated by mechanical dissociation of fresh tissues, and NK cells were extemporaneously analyzed by flow cytometry. We found low frequency of NK cells within control ($2.9 \pm 0.6\%$, 1.47×10^5 NK cells/g) and tumor prostate tissues ($3.6 \pm 0.5\%$ of living lymphocytes, 2.2×10^5 NK cells/g), compared with the proportion of NK cells in peripheral blood ($12.7 \pm 2.3\%$; Fig. 1C). We analyzed NK cell subsets in blood and tissues by flow cytometry, according to CD56 expression (Fig. 1D). We found that the pattern of distribution of CD56^{dim} and CD56^{bright} subsets was significantly perturbed in tumor as well as in control tissues. In peripheral blood from prostate cancer patients, the CD56^{dim} subset prevailed over the CD56^{bright} subset, as described in peripheral blood from healthy donors. In contrast, the CD56^{bright} subset was significantly increased both in control and tumor tissues. Then maturation

and activation markers were measured by flow cytometry (Fig. 2A and B). CD57 has been associated with the terminal differentiation stage of CD56^{dim} NK cells (23) and CD57$^+$ cells displayed higher cytotoxic capacity and decreased capacity to proliferate (24). We found that CD57 expression was significantly reduced in infiltrating NK cells compared with peripheral NK cells. In contrast, the activation markers CD69 and NKp44 were significantly increased in NK cells infiltrating control and tumor tissues compared with pB-PC. To note, CD57 decreased expression was not only due to the lower proportion of CD56^{dim} subset; indeed, CD57 was decreased also within CD56^{dim} subset both in control and tumor tissues. CD69 and NKp44 were mostly increased in CD56^{bright} subset (Fig. 2C).

To further explore prostate-infiltrating NK cells, we measured *ex-vivo* CD107 degranulation of overnight IL2/IL15 activated NK cells in response to K562 erythroleukemia cell line (Fig. 2D and E). Interestingly, NK cells isolated from both control (bottom) and tumor (top) prostate tissues showed significantly low or null degranulation potential (measured as CD107 assay) but high activated phenotype (CD69 expression) compared with peripheral NK cells.

Together, these results show that immature but activated NK cells are overrepresented in prostate gland, regardless of whether the tissue is invaded by the tumor or not. Moreover, prostate-infiltrating NK cells display hyporesponsive functional status in the presence of target cells. This highlights a mechanism of tissue tolerance in prostate gland that impairs NK cell phenotype and functions.

Tumor-induced alterations on activating and inhibitory NK cell receptors

To explore what happens in cancer context, we conducted a comparative analysis between NK cells infiltrating tumor and control prostate tissues (Fig. 3). We found that the activating receptors NKp46 and NKG2D were significantly decreased in NK cells infiltrating tumor compared with control tissues (Fig. 3A). There was also a trend towards a lower expression of NKp30 and DNAM-1 in tumors. In contrast, the inhibitory receptor ILT2 showed higher expression in NK cells infiltrating tumor compared with control tissues (Fig. 3B). Interestingly, CD16, which is involved in antibody-dependent cellular cytotoxicity (ADCC), is clearly decreased in tumor compared with control tissues (Fig. 3C). Representative flow cytometry profiles are shown in Fig. 3D. We observed, as previously published in breast, lung, and colorectal cancer (12, 14, 17), that paired peripheral and intratumoral NK cells from the same patients displayed drastic differences in their phenotype (Supplementary Fig. S1) but our study identifies which ones are due to the tumor and not to tissue localization. We further explored NK cell alterations depending on the stage of prostate cancer: localized (Loc) or locoregional (LCR; i.e., tumor with extracapsular extension, or seminal vesicle/regional lymph node invasion, but has not spread into other organs; $n = 16$), or metastatic prostate cancer for which tumor has already spread to other organs ($n = 4$; see Supplementary Table S1). As depicted in Fig. 3E, the decreased expression of activating NKp46 and NKG2D, and the increased expression of inhibitory ILT2 were more pronounced in NK cells infiltrating metastatic than localized or LCR tumors. These observations prompted us to investigate whether the phenotype of infiltrating NK cells would correlate with clinical outcome. We considered median
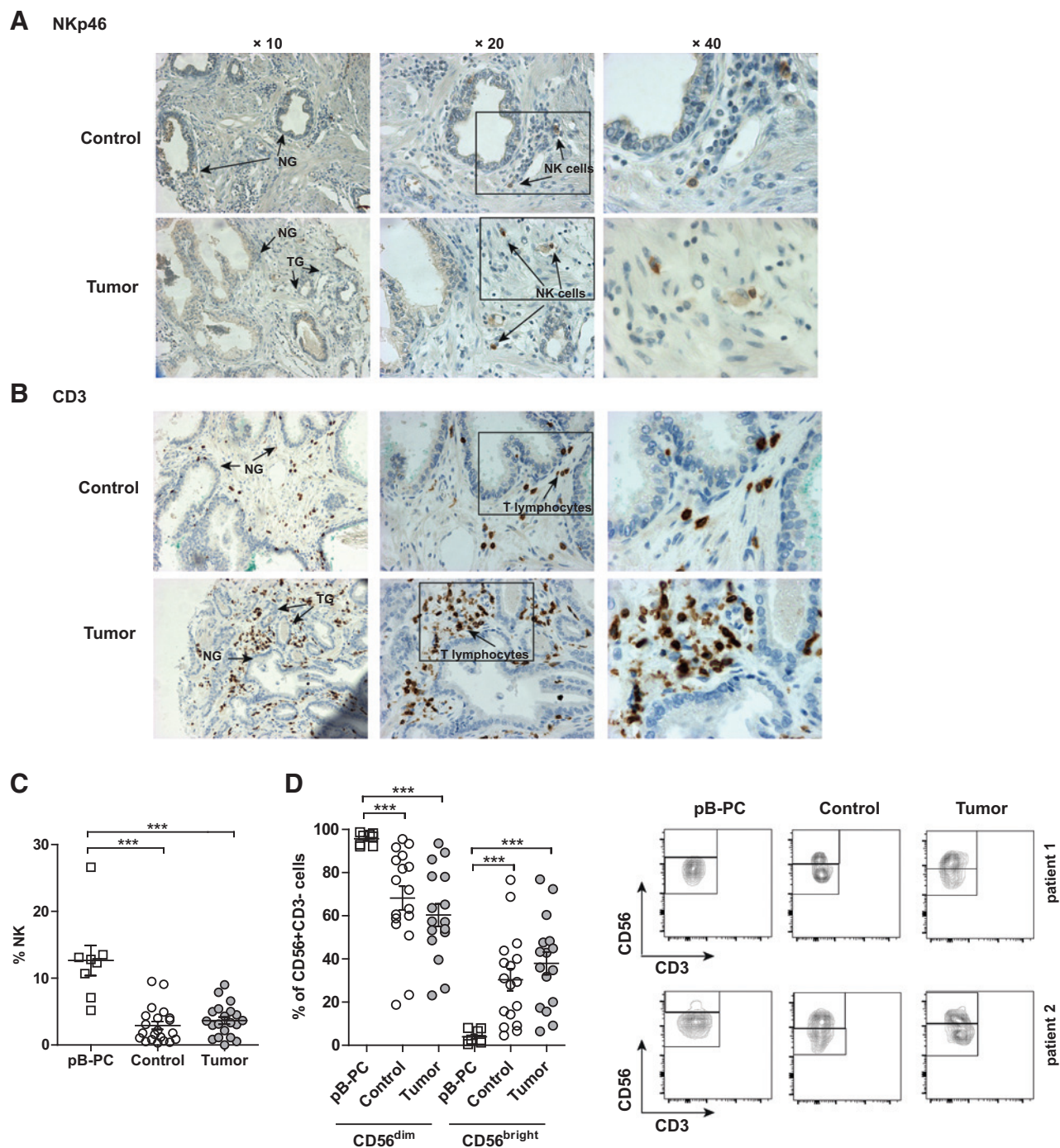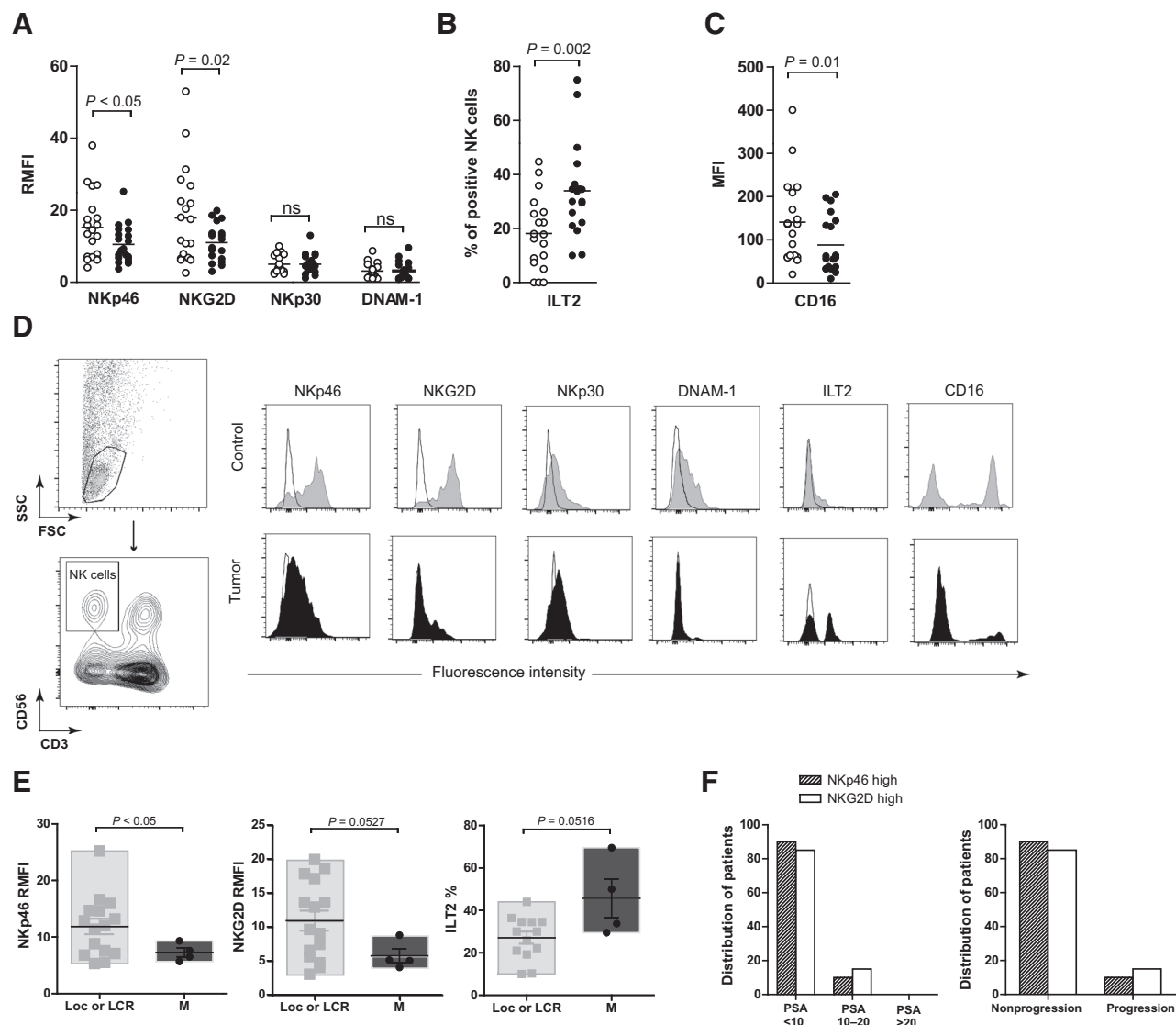
Figure 1.
Frequency and phenotype of NK cell infiltrate in tumor and control prostate tissues. A and B, immunohistochemical staining of infiltrating immune cells on paraffin-embedded control or tumor prostate tissues. A, NKp46^{+} NK cells. B, CD3^{+} T lymphocytes. Brown, positively stained cells. NG, normal prostatic gland; TG, tumor prostatic gland. Original magnifications, ×10, ×20, ×40, followed by computer magnification. C and D, flow cytometry analysis of infiltrating NK cells after tissue dissociation. C, frequency of CD3^{−}CD56^{+} NK cells within prostate tumors ($n = 21$, gray circle) and control prostate tissues ($n = 20$, white circle) gated among living lymphocytes. In parallel, white squares show the frequency of NK cells in peripheral blood from prostate cancer (PC) patients (pB-PC, $n = 10$). The horizontal bar represents the mean value ± SEM. D, frequency of CD56^{dim} and CD56^{bright} NK subsets in tumor and control prostate tissues compared with peripheral blood from patients (pB-PC). The scatter plots (left) report frequency for CD56^{dim} and CD56^{bright} subsets for all patients tested. The horizontal bar represents the mean value ± SEM. Representative examples (right) for flow cytometry gating of CD3^{−}CD56^{+} NK cell subsets are shown in blood, control, and tumor prostate tissues in two patients with prostate cancer. Two regions were selected to represent CD56^{dim} and CD56^{bright} populations. Statistical analyses were done using nonparametric Mann–Whitney test. *, $P < 0.05$; **, $P < 0.01$; ***, $P < 0.001$.
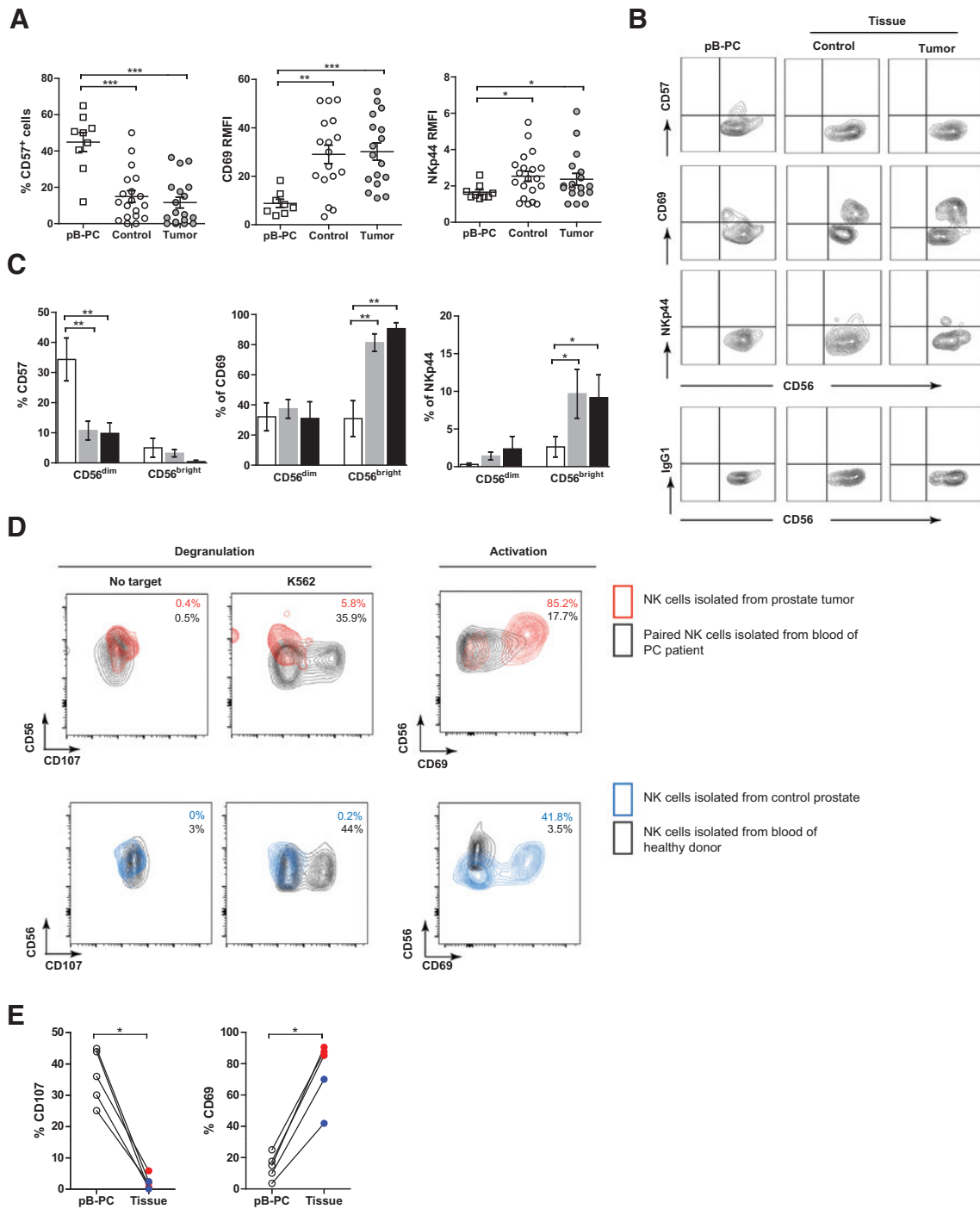
Figure 2.
NK cells infiltrating both control and tumor prostate tissues display altered profile and poor cytotoxic potential. A, expression of CD57, CD69, and NKp44 gated on NK cells isolated from control ($n = 20$, white circle) and tumor prostate tissues ($n = 21$, gray circle) for all patients tested. In parallel, white squares show the expression of each marker on NK cells from peripheral blood (pB-PC, $n = 10$). The horizontal bar represents the mean value $\pm$ SEM. Statistical analyses were done using nonparametric Mann–Whitney test. $*$, $P < 0.05$; $**$, $P < 0.01$; $***$, $P < 0.001$. B, representative dot plots for CD57/CD56, CD69/CD56, and NKp44/CD56 profiles on control and tumor prostate tissues are presented in comparison with peripheral blood. The quadrant marker has been set according to the isotype controls. C, expression of CD57, CD69, and NKp44 on CD56^{dim} and CD56^{bright} NK cell subsets from control (gray column) and tumor (black column) prostate tissues compared with pB-PC (white column). D and E, functionality of NK cells infiltrating control and tumor prostate tissues compared with NK cells from peripheral blood. CD107 degranulation was assessed by flow cytometry on NK cells incubated overnight in medium complemented with IL2 (100 UI/mL) and IL15 (10 ng/mL) before incubation with K562 cell line according to 10:1 E:T ratio for 4 hours. D, dot plot representation of CD107 (degranulation) and CD69 (activation) expression in NK cells infiltrating prostate tumor (red) compared with peripheral NK cells from the same patient (top); and NK cells from control prostate tissue (blue) compared with peripheral NK cells from healthy donor (bottom). Numbers in dot plots indicate the percentage of CD107 or CD69$^+$ cells within CD56$^+$ NK cells. E, summary of CD107 and CD69 expression obtained on NK cells isolated from peripheral blood (white circle) and tissues (control, blue circle; tumor, red circle) Bar graphs represent mean $\pm$ SEM. Statistical analyses were done using nonparametric Mann–Whitney test. $*$, $P < 0.05$; $**$, $P < 0.01$; $***$, $P < 0.001$.

Figure 3.
NK cells infiltrating prostate tumor show specific alterations on activating/inhibitory receptors compared with control tissues. A–D, the expression of activating and inhibitory NK cell receptors was analyzed by flow cytometry on NK cells infiltrating control ($n = 20$, white circle) and tumor ($n = 21$, gray circle) prostate tissues after mechanical dissociation. Scatter dot plots show the expression of activating receptors NKp46, NKG2D, NKp30, DNAM-1 (A); inhibitory receptor ILT2 (B); and cytotoxic molecule CD16 (C) involved in ADCC. The horizontal bar represents the mean value ± SEM. Statistical analyses were done using nonparametric Mann–Whitney test. *, $P < 0.05$; **, $P < 0.01$; ***, $P < 0.001$. D, representative histogram profiles for each receptor expressed on NK cells from control (top) and tumor (bottom) prostate tissues. The gating strategy and isotype controls are shown in the figure. E, expression of NKp46, NKG2D, and ILT2 compared between localized (Loc) or locoregional (LCR) tumors ($n = 16$, gray box plot) and metastatic (M) prostate tumors ($n = 4$, dark box plot). Data are represented as box and whisker (min to max; horizontal lines represent median values) graphs and scatter dot plots. Statistical analyses were done using nonparametric Mann–Whitney test. *, $P < 0.05$; **, $P < 0.01$; ***, $P < 0.001$. F, distribution of patients with high expression of NKp46 (dashed column) or NKG2D (white column) on tumor-infiltrating NK cells according to the measurement of PSA at the time of sample: PSA < 10 ng/mL, PSA comprised between 10 and 20 ng/mL or PSA > 10 ng/mL and the progression or nonprogression of cancer after a median follow-up of 12.1 months. The Fisher exact test was significant ($P < 0.05$).

values for tumor samples ($n = 21$) as cut-off to determine NKp46^{high} (cutoff = 10.6) and NKG2D^{high} (cutoff = 9.9) expression. We looked at the distribution of patients according to their PSA value and clinical status at last follow-up (Fig. 3F). Interestingly, patients with infiltrating NK cells displaying NKp46^{high} (dashed columns) and/or NKG2D^{high} (white columns) expression all belonged to groups with low (<10 ng/mL) to intermediary (comprised between 10 and 20 ng/mL) PSA levels. None of

these patients were found in the poor prognosis group corresponding to high PSA levels. In addition, most patients with high expression of NKp46 and NKG2D on intratumoral NK cells at surgery displayed a high tendency toward no progression 1 year after.

Together, these data show that the tumor specifically targets the balance between activating and inhibitory receptors involved in NK cell cytotoxicity, with underexpression of activating receptors

and overexpression of inhibitory receptors, and more pronounced alterations along with metastatic progression. High expression of NKp46 or NKG2D on infiltrating NK cells correlated with good prognosis, suggesting that NK cells could control tumor escape.

The cytokine milieu in prostate tissue environment impacts NK cell functions partly through TGFβ1

To explore the cytokine environment in prostate gland, we quantified soluble factors released in dissociation supernatant from control and tumor tissues (Fig. 4A and B). We found high levels of TGFβ1, known for its immunosuppressive properties on NK cells, in control supernatants and the secretion was significantly increased in the tumor. PGE2 secretion was also increased in tumor compared with control milieu. Other sol-

uble factors such as Rantes and IL8 were found in tumor milieu and may account for inflammatory signals observed in cancer context. Then, NK cells from healthy donors were exposed to dissociation supernatants from control or tumor tissues for 24 hours to test the effect of cytokine environment on NK cells (Fig. 4C and D). We found that cytokine milieu from tumor induced a profound inhibition of CD107 degranulation compared with control supernatants. Finally, blocking TGFβ1 efficiently restored CD107 degranulation in control condition (by 63% on average) but only partially when NK cells were exposed to tumor supernatants (by 18%). Our results show that cytokine milieu in the prostate gland contains immunosuppressive soluble factors, including TGFβ1, that can affect NK cell functions. These observations further strengthen and reproduce the
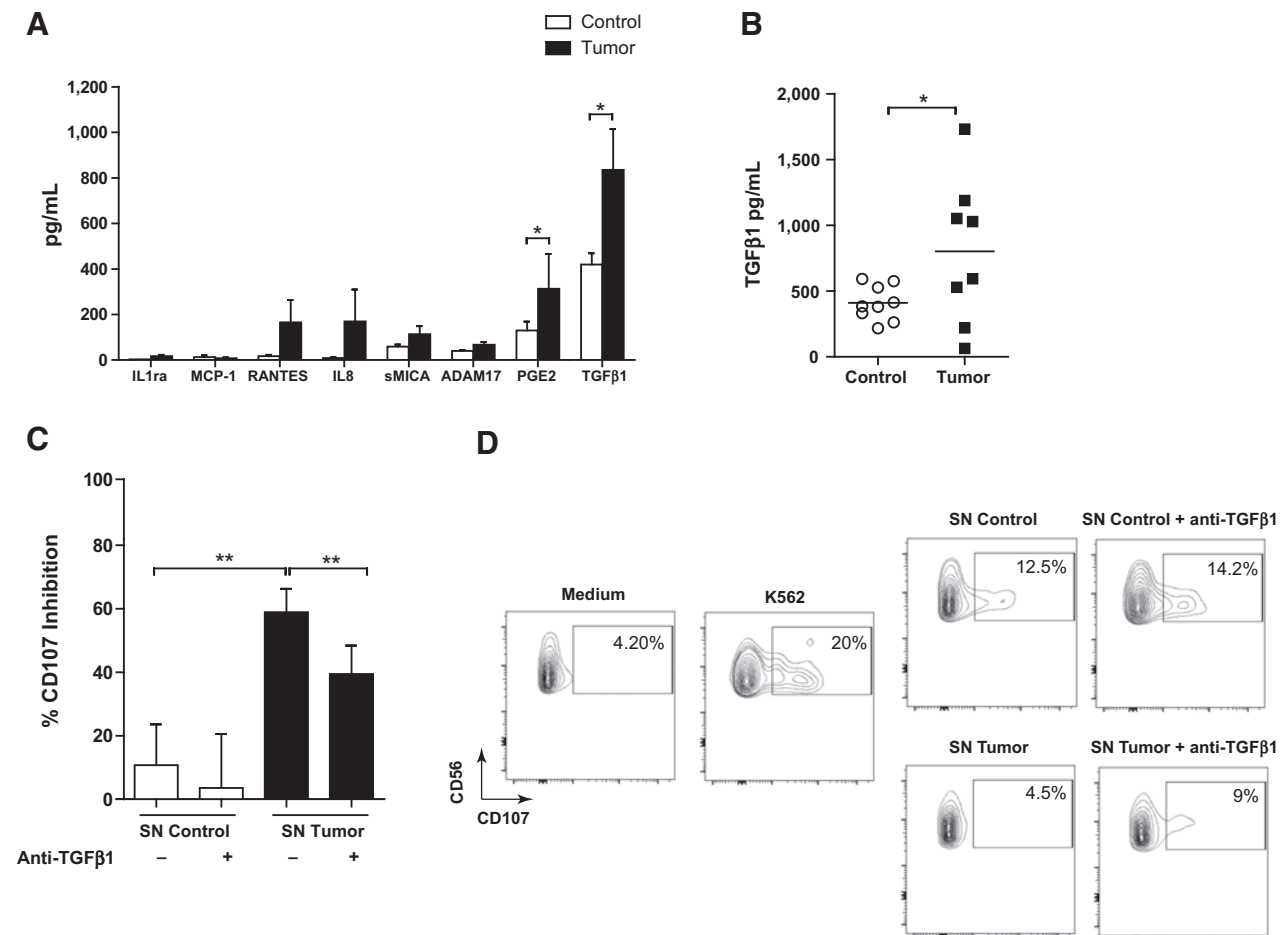
Figure 4.
Analysis of cytokine milieu in control and tumor prostate tissues. A, soluble factor production in dissociation supernatant from control (white column, $n = 8$) and tumor (black column, $n = 8$) prostate tissues. The histograms represent the secretion of IL1ra, MCP-1, RANTES, IL8, evaluated by multiplex assays, and sMICA, ADAM17, PGE2, TGFβ1, evaluated by ELISA, as mean ± SEM. The levels of cytokines have been corrected for cell number after tissue dissociation and are represented as pg/mL for 1 million of cells. B, scatter dot plot representation of TGFβ1 secretion (pg/mL for 1 million of cells) in supernatants from control and tumor prostate tissues by ELISA. Data are shown as mean ± SEM. Statistical analyses were done using nonparametric Mann–Whitney test. *, $P < 0.05$; **, $P < 0.01$; ***, $P < 0.001$. C, impact of the cytokine milieu on NK cells. Peripheral NK cells from three independent healthy donors were exposed for 24 hours to individual dissociation supernatants (dilution one-fourth) from control ($n = 6$) or tumor ($n = 5$) prostate tissues. To evaluate the role of TGFβ1, dissociation supernatants were preincubated in parallel with neutralizing TGFβ1 antibody (10 μg/mL) for 30 minutes before exposure to NK cells. NK degranulation was assessed against K562 cell line in a 4-hour assay (E:T ratio = 1:1) and the percentage of NK cells positive for CD107 was analyzed by flow cytometry. Data are shown as the percentage of CD107 inhibition calculated as [% positive control (without supernatant) − % in the condition with supernatant]/% positive control × 100 ± SEM. Statistical analyses were done using Mann–Whitney test. *, $P < 0.05$; **, $P < 0.01$; ***, $P < 0.001$. D, representative flow cytometry analyses of CD107 degranulation after exposure to supernatant from control or prostate tissue, and recovery of degranulation after TGFβ1 blockade. The gate has been set according to medium condition without K562 target cell line.

low or null degranulation potential of NK cells isolated from control and tumor tissues (Fig. 2D).

Prostate cancer cells alter the receptors involved in their recognition

To explore the mechanism that may account for phenotypical differences between NK cells infiltrating control and tumor tissues, we performed transwell coculture experiments with PC3 prostate cancer cell line (Fig. 5A). NK cells from healthy donors were exposed to PC3 cell line through direct or indirect (through transwell membrane) contact for 48 hours. We found that PC3 cells induced a significant downregulation of NKp46, NKG2D, and DNAM-1 after cell-to-cell contact (Fig. 5B). There was also a trend towards a decreased expression of NKp30 and CD16. In contrast, ILT2 (inhibitory receptor) and CD69 (activation marker)

expression on NK cells were significantly higher after contact with PC3 cell line.

Because NK cell cytotoxicity is known to depend on the engagement of different triggering receptors, we screened the expression of ligands for NK cell receptors on PC3 cell line (Fig. 5C). PC3 cells expressed high level of ligands for DNAM-1 (Nectin-2 and CD155/PVR). The expression of ligands for NKG2D was heterogeneous (detection with antibodies against MICA/B and ULBP1/2/3, or with NKG2D-Fc recombinant protein). In contrast, NKp30-ligand and NKp46-ligand expression were relatively weak, but Fc-fusion proteins have lower affinity than that of specific mAbs. The expression of HLA family molecules was heterogeneous. To assess the specific involvement of NK cell receptors during the recognition of prostate tumor cells, we preincubated resting NK cells from healthy donors with blocking
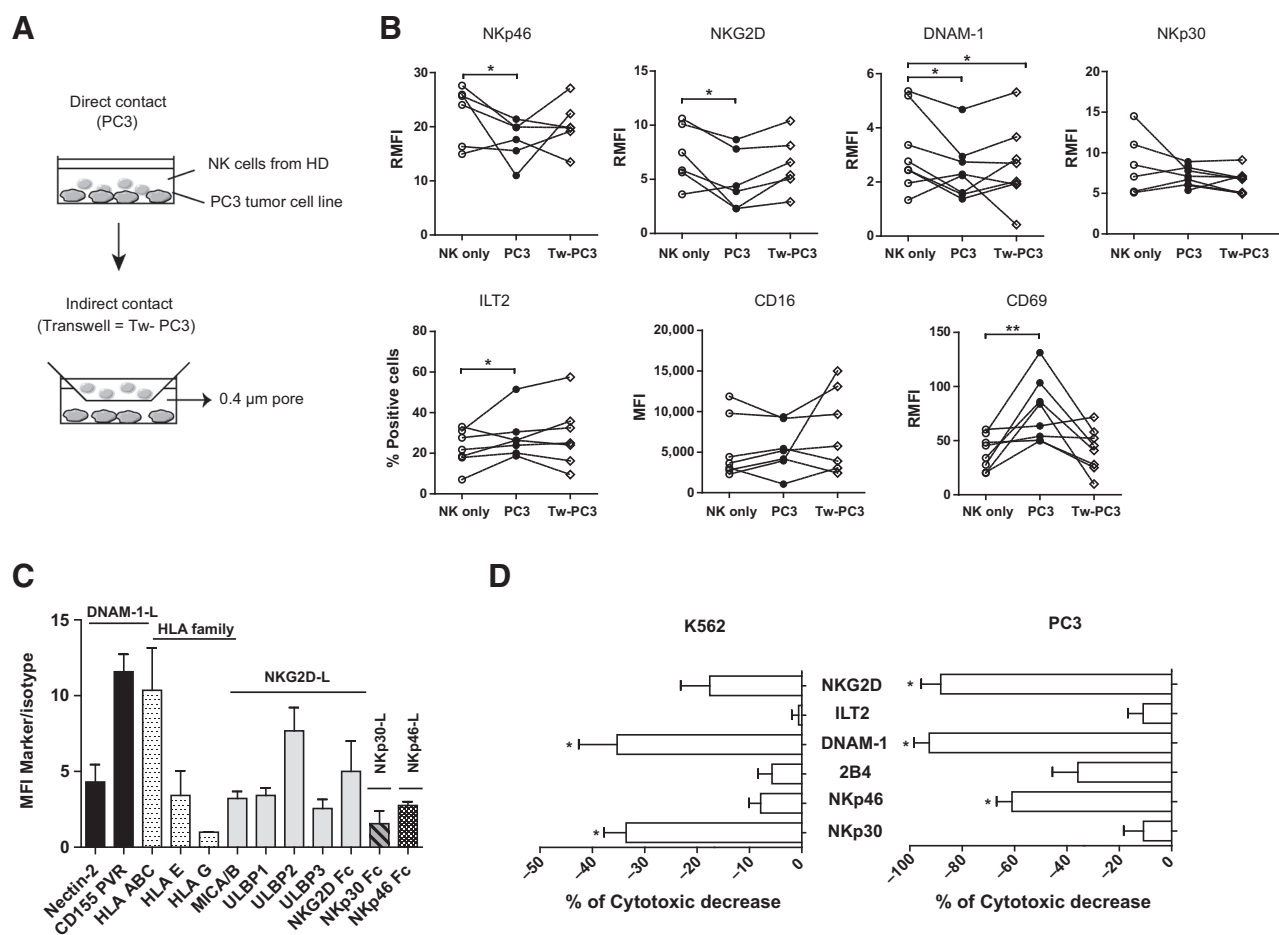
Figure 5.
Prostate tumor cells alter the expression of activating/inhibitory NK cell receptors through direct contact. A, peripheral PBMCs from healthy donors were exposed to PC3 prostate cell line through direct or indirect (Tw-PC3 for "transwell membrane," Greiner Bio One, 0.4 μm) contact, according to a 10:1 E:T ratio. After 48 hours, NK cells were harvested and phenotyped for NK cell receptors by flow cytometry. B, the graphs show the expression of NK cell receptors on NK cells exposed to PC3 prostate tumor cell line directly or through transwell membrane, compared with nonexposed NK cells. Results are representative of three independent experiments ($n = 7$ healthy donors in total). Statistical analyses were done using nonparametric Wilcoxon matched-pairs signed rank test. *, $P < 0.05$; **, $P < 0.01$; ***, $P < 0.001$. C, expression of NK cell ligands on PC3 prostate cell line by flow cytometry for three independent experiments. Bar graphs report the expression of ligands for DNAM-1, NKG2D, NKp30, NKp46, and the expression of HLA molecules. Data are shown as mean ± SEM. D, cytotoxicity of resting NK cells against PC3 (right) or K562 cell line (positive control, left) was evaluated in a 4-hour ^{51}Cr assay in the presence of blocking antibodies for NKp30, NKp46, 2B4, DNAM-1, ILT2, NKG2D, or irrelevant isotype control mAb. Target cell lysis was measured by Cr51 release. Results are shown as the percentage of cytotoxic decrease induced by the blocking antibodies compared with the irrelevant control mAb on three independent experiments. Statistical analyses were done using nonparametric Wilcoxon matched-pairs signed rank test. *, $P < 0.05$; **, $P < 0.01$; ***, $P < 0.001$.

antibodies to NK cell receptors, and then used them in a ^{51}Cr cytotoxic assay against PC3 or K562 cell lines (Fig. 5D). We found that blocking NKp46, DNAM-1, or NKG2D significantly decreased the cytotoxicity of NK cells against the PC3 cell line. Blocking NKp30 decreased cytotoxicity to a lower extent, corroborating NKp30 ligand expression. As a control, NKp30, DNAM-1, and to a lesser extent NKG2D were the major receptors involved in NK cell cytotoxicity against K562 cell line, as described in the literature. In conclusion, our findings show that prostate cancer cells downregulate the activating receptors involved in their recognition, by mechanism dependent on cell-to-cell contact. Interestingly, these are precisely the receptors we found dysregulated in human prostate tumors. Mechanistically, we found an increased pool of intracellular NKp46 in NK cells isolated from tumors compared with peripheral NK cells, suggesting that NKp46 could be internalized but not degraded in response to its ligand in tumor (Supplementary Fig. S2A). We did not detect intracellular NKG2D, but sMICA ($^*P < 0.05$) was significantly increased in sera from prostate cancer patients compared with healthy donors, and sMICB ($^{**}P < 0.01$) was significantly increased in patients with metastatic disease stage, thus shedding of MICs could lead to internalization and degradation of NKG2D (Supplementary Fig. S2B).

Peripheral NK cells from metastatic patients reflect the intratumoral alterations

To strengthen these observations, we enlarged our analysis to blood samples from patients with localized prostate cancer (Loc, $n = 18$), metastatic prostate cancer (Meta, $n = 30$), and healthy donors as controls (HD, $n = 20$; Fig. 6A). The expression of activating receptors NKp46 and NKG2D was significantly lower in patients with metastatic prostate cancer than in patients with localized prostate cancer or HD. There was also a trend towards a decreased expression of NKp30 and DNAM-1 in metastatic compared with localized prostate cancer patients. In contrast, the expression of inhibitory receptor ILT2 was significantly upregulated in metastatic prostate cancer patients compared with localized patients or HD. Hence, NK cells from peripheral blood of metastatic prostate cancer patients reflect the same phenotypic alterations, targeted on NKp46, NKG2D, and ILT2 than NK cells infiltrating the tumor site. In line with this point, intratumoral NKp46 expression was positively correlated with paired peripheral NKp46 expression from the same patients ($n = 7$; $R = 0.56$, $P = 0.07$; Fig. 6B). We submitted the median expression of each marker for each group to TMEV software representation (Fig. 6C), which clearly emphasized that localized patients showed an intermediary phenotype, whereas the metastatic group displayed an inverted profile compared with HD. Kruskal–Wallis ANOVA analysis found that NKp46, NKG2D, and ILT2 significantly discriminated HD, localized, and metastatic prostate cancer patients. Other inhibitory receptors such as NKG2A and CD158b (KIR family) were increased in prostate cancer patients compared with HD. The upregulation of NKp44 in peripheral NK cells from metastatic patients showed that these cells were indeed activated. Interestingly, NKp46 expression in blood from prostate cancer patients was significantly inversely correlated with PSA measurement ($P < 0.01$) at sample, the major clinical marker of poor prognosis in prostate cancer, and Gleason score (Fig. 6D).

We next assessed the functionality of overnight IL2/IL15 activated peripheral NK cells from prostate cancer patients through their capacity to degranulate (CD107 positivity). We found that degranulation efficiency was significantly reduced in localized and metastatic prostate cancer patients compared with HD (Fig. 6E), and that CD107 response was positively correlated with NKp46 ($R = 0.51$, $P = 0.0002$) and NKp30 ($R = 0.50$, $P = 0.0002$) expression at the surface of NK cells (Fig. 6F). IFNγ and TNFα production were also reduced in patients compared with HD (Supplementary Fig. S3A). NK cells that can exert multiple functions, in contrast with monofunctional NK cells, are more potent effector cells (25). Thus, we looked at the multifunctional potential of peripheral NK cells using the Boolean gating strategy. We found that NK cells from metastatic prostate cancer patients were mostly monofunctional cells, exerting CD107 degranulation or IFNγ or TNFα production, than NK cells from localized prostate cancer patients or HD (Supplementary Fig. S3A). Redirected lysis against P815 target cell line using anti-CD16, anti-NKp30, or anti-NKp46 antibody was also reduced in prostate cancer patients compared with healthy donors (Supplementary Fig. S3B). Finally, effective killing of K562 cell line was significantly reduced in resting NK cells from metastatic prostate cancer patients compared with localized prostate cancer patients or HD (Fig. 6G). Altogether these results show that phenotypic alterations of peripheral NK cells in metastatic prostate cancer are associated with major impaired functions.

Discussion

Our study highlights a peculiar pattern where CD56^{bright} subset is increased in the prostate gland, suggesting an immature but activated phenotype compared with blood. NK cells infiltrating control and tumor prostate tissues are not able to exert potent functionality by ex vivo exposure to tumor cells, and this was reproduced by cytokine milieu, strengthening the tolerogenic environment in the prostate gland. This pattern was not observed in previous studies: CD56^{bright}CD16$^-$ cells were found to be enriched in lung and breast cancer (16, 26) but NK cells infiltrating healthy lung or breast shared more similarities with blood NK cells (12, 14). A recent report showed that NK cell subset distribution is organ specific, with CD56^{bright} predominant in liver, adrenal gland, colorectal tissues, and CD56^{dim} predominant in lung and breast tissues (27). One hypothesis is that prostate gland appears to be poorly infiltrated by immune cells at basal level; thus, immune infiltration would rather be related to intraprostatic inflammation. Thus, the phenotype observed could be a consequence of NK cell attraction from the periphery and subsequent activation. Indeed, the enrichment of CD56^{bright} subset suggests either that this subset is specifically attracted from the periphery to organs, or that the tissue environment can have an influence, that is block or reverse the maturation of NK cells. In either scenario, our data suggest that NK cells infiltrating prostate gland would be poorly armed in case of tumor development. We found that TGFβ1, known to alter lymphocyte functions (28), is secreted in high amounts in normal prostate and increased in cancer. Interestingly, a higher expression of TGFβ1 was observed by qRT-PCR in prostate tumors with higher Gleason scores (29). In the literature, it has been shown that the uterine decidua is populated by CD16$^-$ NK cells (30), and that TGFβ1 results in conversion of CD16$^+$ into CD16$^-$ cells in vitro, highlighting the influence of TGFβ1 on the genesis of NK subsets (30, 31). Specific expansion of circulating CD56$^{bright/dim}$CD16$^-$ NK cells has been reported in metastatic melanoma; and this increase was associated with

Pasero et al.
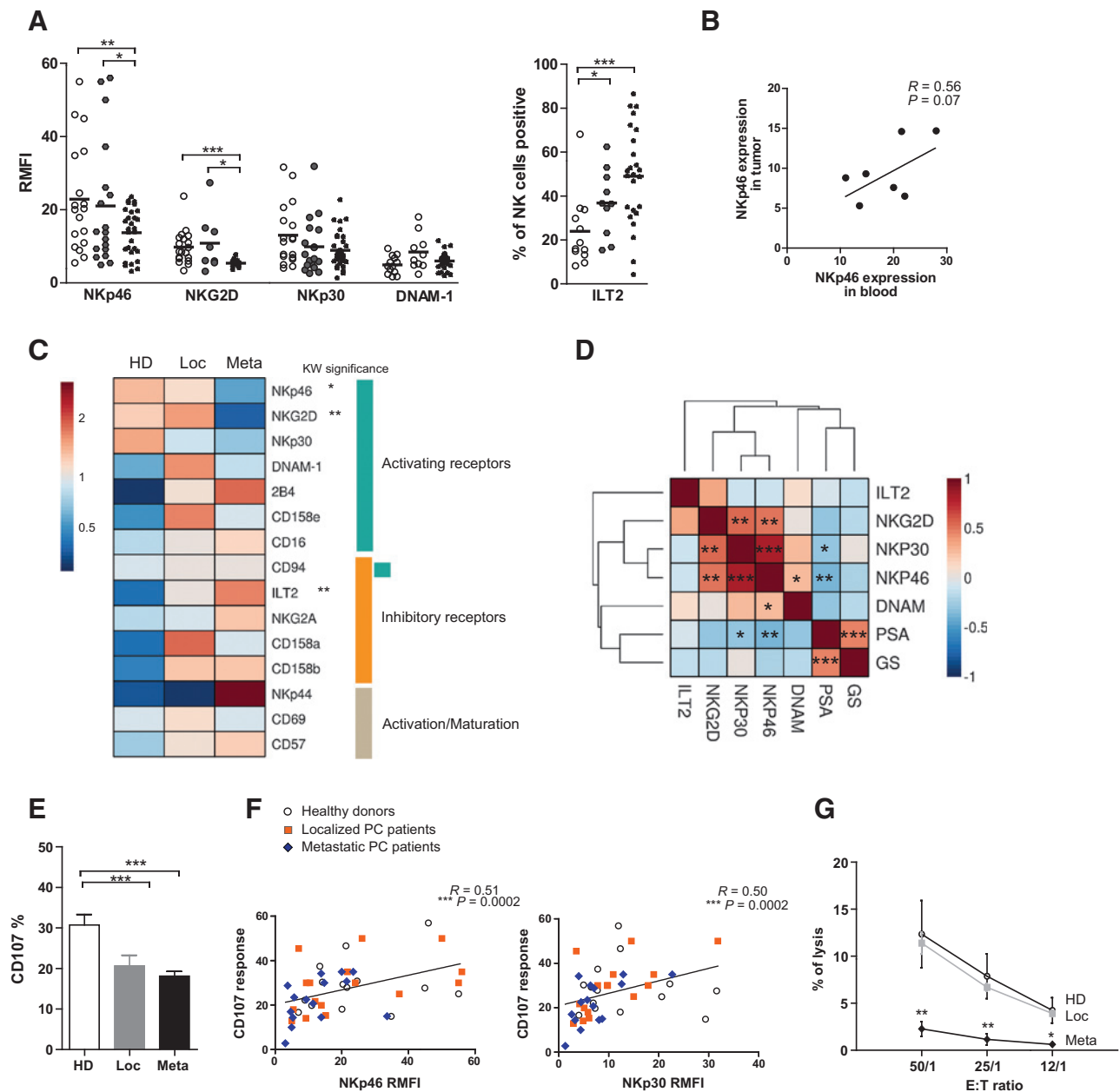
Figure 6.
Peripheral blood NK cells are tumor-induced subsets with altered phenotype and functions. A, NK cells were collected from blood samples of patients with localized ($n = 18$, gray circle) and metastatic prostate cancer (PC; $n = 30$, black circle) and were compared with NK cells from healthy donors ($n = 20$, white circle) by flow cytometry. Scatter dot plots report the expression of NKp46, NKG2D, NKp30, DNAM-1 (as MFI ratio compared with isotypic control) and ILT2 (as the percentage of positive NK cells for the marker). The horizontal bar represents the mean value. B, Spearman correlation between the intratumoral expression of NKp46 and the expression in peripheral blood from the same patients. C, summary of the median expression of the 15 NK cell receptors tested in blood of patients with prostate cancer compared with HD. Values represent the ratio between the median value for given marker in a group compared with the median value in all groups included. Statistical analyses were done using Kruskal–Wallis (KW) ANOVA. *, $P < 0.05$; **, $P < 0.01$; ***, $P < 0.001$. D, correlation between the expression of NK-cell receptors in peripheral blood and the clinical parameters (GS, PSA) for patients with prostate cancer. The vertical bar represents the Spearman correlation coefficients and the P values are indicated in each case if correlation was significant. E, CD107 degranulation of peripheral NK cells isolated from patients with localized ($n = 13$, gray column) or metastatic prostate cancer ($n = 23$, black column), compared with NK cells from healthy donors (HD; $n = 18$, white column). Overnight IL2/IL15-activated NK cells were incubated with K562 target cell line according to 1:1 E/T ratio for 4 hours, and CD107 expression was assessed by flow cytometry. Data are shown as mean ± SEM. F, Spearman correlation of CD107 response with the expression of NKp46 and NKp30 in peripheral NK cells. Each dot is coded for healthy donors (white circle), localized (orange square), or metastatic patients with prostate cancer (PC; blue diamond). Spearman correlation coefficients and P values are indicated. G, the cytotoxicity of resting NK cells from patients with prostate cancer was evaluated in a 4-hour ^{51}Cr assay against K562 cell line (E:T ratio = 1:1) and compared with healthy donors (HD). Target cell lysis was measured by Cr51 release. Statistical analyses were done using nonparametric Mann–Whitney test. *, $P < 0.05$; **, $P < 0.01$; ***, $P < 0.001$.

elevated plasma TGFβ1 (32). Besides alterations on NK cell subsets, TGFβ1 can induce the downregulation of NKG2D and NKp30 expression on NK cells, leading to a decreased ability of NK cells to kill target cells (33). Phase I studies with fresolimumab (human anti-TGFβ mAb) are currently ongoing in melanoma and renal cell carcinoma (34) and our findings strongly suggest that clinical strategies targeting TGFβ1 could be of major interest in prostate cancer. Interestingly, we extracted mRNA expression from a public database including 498 localized prostate tumors, and we found that TGFβ1 was positively correlated with some markers of tumor aggressiveness in prostate cancer such as Gleason score, residual tumor, and pathologic T (Supplementary Fig. S4). CD57 was inversely correlated with Gleason score and pathologic T, sustaining that lack of maturity of immune cells, and consequently lack of cytotoxic functions are associated with aggressive prostate cancer disease.

Besides this first level of tissue tolerance, prostate cancer cells induce specific alterations on activating (NKp46, NKG2D) and inhibitory (ILT2) receptors involved in cytotoxicity. Interestingly, our study points out that the receptors involved in cancer recognition are specific according to the tumor type: here, we identify NKp46, NKG2D, and DNAM-1 as the main receptors involved in the killing of prostate cancer cells. In melanoma, NKp30, NKp44, and NKG2D are the receptors modulated by coculture of NK cells with melanoma cell lines (10, 35). In non–small cell lung carcinoma, a cluster of five receptors (NKp30, DNAM-1, NKp80, CD16, and ILT-2) was reduced in intratumoral NK cells. In breast cancer, the main receptors involved in NK cell cytotoxicity are DNAM-1 and NKG2D (13). Hence, prostate tumor cells could escape from NK cell antitumor immunity by altering the phenotype of NK cells and by decreasing their cytotoxic potential, as observed in several malignancies (11, 35–38). The molecular mechanisms underlying the receptor downmodulation could either be chronic ligand exposure (38), or cytokine-induced downregulation. Peripheral NK cells reflect these phenotypic and functional alterations and may represent tumor-induced subsets as reported in breast cancer (26). In line with these results, impaired NK cell activity measured as IFNγ levels has been recently described in blood from prostate cancer patients (39). To note, we found an overexpression of NKp44 that might seem contrary to what would be expected for an activating receptor but this upregulation was also observed in breast and lung cancer (12, 14), and seems rather be a hallmark of NK cell activation. Interestingly, it has been recently described that NKp44 recognizes two distinct ligands resulting in either activation or inhibition of NK cell effector responses in response to tumor cells (40). Our study provides evidence for the importance of NKp46 and NKG2D in human prostate cancer. The involvement of NKG2D in prostate cancer has been explored in animal models: NKG2D-deficient transgenic adenocarcinoma of the mouse prostate (TRAMP) mice develop more aggressive prostate tumor than NKG2D^{WT} TRAMP counterparts (5). In humans, MIC is widely expressed in prostate adenocarcinoma; however, significant serum levels of soluble MIC were observed in patients with advanced prostate cancer, indicating that prostate tumors may counteract NKG2D-mediated immunity via MIC shedding (41, 42). Ligands for NKG2D (MICA/B and ULBP1) are expressed on circulating monocytes from prostate cancer patients and could be responsible for NKG2D downregulation on NK cells (43). This is the first time to our knowledge that the major role of NKp46 in

prostate cancer is pointed out. Therefore, counteracting tumor-induced downregulation of surface NKp46 and NKG2D or sustaining NKp46 and NKG2D-mediated immune response could represent new therapeutic option for metastatic prostate cancer patients. We have recently retrospectively studied a cohort of metastatic prostate cancer patients, highlighting an association between NK cell markers in blood, including NKp46, and clinical outcomes (44).

Importantly, it has been shown that some treatments in prostate cancer can affect the immune infiltrate: ADT increases significantly the infiltration of CD3$^+$ and CD8$^+$ T lymphocytes, as well as CD68$^+$ macrophages within the tumor (22). Systemic administration of Sipuleucel-T prior to radical prostatectomy increases CD3$^+$, CD4$^+$, FoxP3$^-$, CD8$^+$ T cells in tissues compared with pretreatment biopsies (45). These observations together with our findings suggest that combined treatments to increase the recruitment of immune infiltrate, and to restore NK cell efficiency at the same time could represent promising approach in prostate cancer. Furthermore, our data show a decreased expression of CD16 on intratumoral NK cells, suggesting that the ability to perform ADCC would be compromised as confirmed by redirect lysis results on peripheral NK cells from prostate cancer patients. Thus, preventing CD16 downregulation or shedding could improve the efficacy of therapeutic antibody-mediated effects.

Through an integrative view of the literature, it seems obvious that prostate cancer builds a strong immunosuppressive microenvironment: the tumor cells may recruit and facilitate the accumulation of Treg and TH17 lymphocytes (46, 47), which, in turn, could suppress the antitumor immunity; the CD8$^+$ T cells infiltrating prostate tumors become tolerized (48) and are induced to become suppressor cells (49); and here we demonstrate that NK cells are switched toward a noncytotoxic profile. Interestingly, these events are all mediated in part through TGFβ1. To our knowledge, this is the first report demonstrating multiple levels of tolerance to NK cells in a solid tumor, with tissue- and tumor-induced alterations, that together strongly impair NK cell antitumor immunity in prostate cancer. Besides shedding light on the phenotype and functions of prostate-infiltrating NK cells in normal and tumor context, our data pave the way for developing therapies aimed to restore NK cell efficiency in the prostate tumor microenvironment.

Disclosure of Potential Conflicts of Interest

Authors' Contributions

Conception and design: C. Pasero, G. Gravis, P. Rocchi, M. Paciencia-Gros, F. Poizat, A. Moretta, D. Olive
Development of methodology: C. Pasero, G. Gravis, M. Paciencia-Gros, F. Poizat, D. Olive
Acquisition of data (provided animals, acquired and managed patients, provided facilities, etc.): C. Pasero, G. Gravis, M. Guerin, J. Thomassin-Piana, M. Paciencia-Gros, F. Poizat, M. Bentobji, J. Walz, N. Salem, S. Brunelle, D. Olive
Analysis and interpretation of data (e.g., statistical analysis, biostatistics, computational analysis): C. Pasero, G. Gravis, S. Granjeaud, P. Rocchi, M. Paciencia-Gros, F. Poizat, M. Bentobji,. Salem, S. Brunelle, A. Moretta, D. Olive
Writing, review, and/or revision of the manuscript: C. Pasero, G. Gravis, M. Guerin, M. Paciencia-Gros, F. Poizat, J. Walz, A. Moretta, D. Olive

References

1. Jemal A, Murray T, Ward E, Samuels A, Tiwari RC, Ghafoor A, et al. Cancer statistics, 2005. CA Cancer J Clin 2005;55:10–30.
2. May KFJr, Gulley JL, Drake CG, Dranoff G, Kantoff PW. Prostate cancer immunotherapy. Clin Cancer Res 2011;17:5233–8.
3. Fridman WH, Pages F, Sautes-Fridman C, Galon J. The immune contexture in human tumours: impact on clinical outcome. Nat Rev Cancer 2012;12:298–306.
4. Vivier E, Tomasello E, Baratin M, Walzer T, Ugolini S. Functions of natural killer cells. Nat Immunol 2008;9:503–10.
5. Guerra N, Tan YX, Joncker NT, Choy A, Gallardo F, Xiong N, et al. NKG2D-deficient mice are defective in tumor surveillance in models of spontaneous malignancy. Immunity 2008;28:571–80.
6. Imai K, Matsuyama S, Miyake S, Suga K, Nakachi K. Natural cytotoxic activity of peripheral-blood lymphocytes and cancer incidence: an 11-year follow-up study of a general population. Lancet 2000;356:1795–9.
7. Hanna J, Bechtel P, Zhai Y, Youssef F, McLachlan K, Mandelboim O. Novel insights on human NK cells' immunological modalities revealed by gene expression profiling. J Immunol 2004;173:6547–63.
8. Moretta A, Bottino C, Vitale M, Pende D, Cantoni C, Mingari MC, et al. Activating receptors and coreceptors involved in human natural killer cell-mediated cytolysis. Annu Rev Immunol 2001;19:197–223.
9. Rabinovich GA, Gabrilovich D, Sotomayor EM. Immunosuppressive strategies that are mediated by tumor cells. Annu Rev Immunol 2007;25:267–96.
10. Balsamo M, Scordamaglia F, Pietra G, Manzini C, Cantoni C, Boitano M, et al. Melanoma-associated fibroblasts modulate NK cell phenotype and antitumor cytotoxicity. Proc Natl Acad Sci U S A 2009;106:20847–52.
11. Costello RT, Sivori S, Marcenaro E, Lafage-Pochitaloff M, Mozziconacci MJ, Reviron D, et al. Defective expression and function of natural killer cell-triggering receptors in patients with acute myeloid leukemia. Blood 2002;99:3661–7.
12. Mamessier E, Sylvain A, Thibult ML, Houvenaeghel G, Jacquemier J, Castellano R, et al. Human breast cancer cells enhance self tolerance by promoting evasion from NK cell antitumor immunity. J Clin Invest 2011;121:3609–22.
13. Mamessier E, Sylvain A, Bertucci F, Castellano R, Finetti P, Houvenaeghel G, et al. Human breast tumor cells induce self-tolerance mechanisms to avoid NKG2D-mediated and DNAM-mediated NK cell recognition. Cancer Res 2011;71:6621–32.
14. Platonova S, Cherfils-Vicini J, Damotte D, Crozet L, Vieillard V, Validire P, et al. Profound coordinated alterations of intratumoral NK cell phenotype and function in lung carcinoma. Cancer Res 2011;71:5412–22.
15. Gillard-Bocquet M, Caer C, Cagnard N, Crozet L, Perez M, Fridman WH, et al. Lung tumor microenvironment induces specific gene expression signature in intratumoral NK cells. Front Immunol 2013;4:19.
16. Carrega P, Morandi B, Costa R, Frumento G, Forte G, Altavilla G, et al. Natural killer cells infiltrating human nonsmall-cell lung cancer are enriched in CD56 bright CD16(-) cells and display an impaired capability to kill tumor cells. Cancer 2008;112:863–75.
17. Rocca YS, Roberti MP, Arriaga JM, Amat M, Bruno L, Pampena MB, et al. Altered phenotype in peripheral blood and tumor-associated NK cells from colorectal cancer patients. Innate Immun 2013;19:76–85.
18. Schleypen JS, Baur N, Kammerer R, Nelson PJ, Rohrmann K, Grone EF, et al. Cytotoxic markers and frequency predict functional capacity of natural killer cells infiltrating renal cell carcinoma. Clin Cancer Res 2006;12:718–25.
19. Rusakiewicz S, Semeraro M, Sarabi M, Desbois M, Locher C, Mendez R, et al. Immune infiltrates are prognostic factors in localized gastrointestinal stromal tumors. Cancer Res 2013;73:3499–510.
20. Delahaye NF, Rusakiewicz S, Martins I, Menard C, Roux S, Lyonnet L, et al. Alternatively spliced NKp30 isoforms affect the prognosis of gastrointestinal stromal tumors. Nat Med 2011;17:700–7.
21. Arnon TI, Markel G, Bar-Ilan A, Hanna J, Fima E, Benchetrit F, et al. Harnessing soluble NK cell killer receptors for the generation of novel cancer immune therapy. PLoS One 2008;3:e2150.
22. Gannon PO, Poisson AO, Delvoye N, Lapointe R, Mes-Masson AM, Saad F. Characterization of the intra-prostatic immune cell infiltration in androgen-deprived prostate cancer patients. J Immunol Methods 2009;348:9–17.
23. Bjorkstrom NK, Riese P, Heuts F, Andersson S, Fauriat C, Ivarsson MA, et al. Expression patterns of NKG2A, KIR, and CD57 define a process of CD56dim NK-cell differentiation uncoupled from NK-cell education. Blood 2010;116:3853–64.
24. Lopez-Verges S, Milush JM, Pandey S, York VA, Arakawa-Hoyt J, Pircher H, et al. CD57 defines a functionally distinct population of mature NK cells in the human CD56dimCD16+ NK-cell subset. Blood 2010;116:3865–74.
25. Bryceson YT, Fauriat C, Nunes JM, Wood SM, Bjorkstrom NK, Long EO, et al. Functional analysis of human NK cells by flow cytometry. Methods Mol Biol 2010;612:335–52.
26. Mamessier E, Pradel LC, Thibult ML, Drevet C, Zouine A, Jacquemier J, et al. Peripheral blood NK cells from breast cancer patients are tumor-induced composite subsets. J Immunol 2013;190:2424–36.
27. Carrega P, Bonaccorsi I, Di Carlo E, Morandi B, Paul P, Rizzello V, et al. CD56(bright)perforin(low) noncytotoxic human NK cells are abundant in both healthy and neoplastic solid tissues and recirculate to secondary lymphoid organs via afferent lymph. J Immunol 2014;192:3805–15.
28. Flavell RA, Sanjabi S, Wrzesinski SH, Licona-Limon P. The polarization of immune cells in the tumour environment by TGFbeta. Nat Rev Immunol 2010;10:554–67.
29. Reis ST, Pontes-Junior J, Antunes AA, Sousa-Canavez JM, Abe DK, Cruz JA, et al. Tgf-beta1 expression as a biomarker of poor prognosis in prostate cancer. Clinics 2011;66:1143–7.
30. Keskin DB, Allan DS, Rybalov B, Andzelm MM, Stern JN, Kopcow HD, et al. TGFbeta promotes conversion of CD16+ peripheral blood NK cells into CD16- NK cells with similarities to decidual NK cells. Proc Natl Acad Sci U S A 2007;104:3378–83.
31. Allan DS, Rybalov B, Awong G, Zuniga-Pflucker JC, Kopcow HD, Carlyle JR, et al. TGF-beta affects development and differentiation of human natural killer cell subsets. Eur J Immunol 2010;40:2289–95.

32. Holtan SG, Creedon DJ, Thompson MA, Nevala WK, Markovic SN. Expansion of CD16-negative natural killer cells in the peripheral blood of patients with metastatic melanoma. Clin Dev Immunol 2011;2011: 316314.

33. Castriconi R, Cantoni C, Della Chiesa M, Vitale M, Marcenaro E, Conte R, et al. Transforming growth factor beta 1 inhibits expression of NKp30 and NKG2D receptors: consequences for the NK-mediated killing of dendritic cells. Proc Natl Acad Sci U S A 2003;100:4120–5.

34. Morris JC, Tan AR, Olencki TE, Shapiro GI, Dezube BJ, Reiss M, et al. Phase I study of GC1008 (fresolimumab): a human anti-transforming growth factor-beta (TGFbeta) monoclonal antibody in patients with advanced malignant melanoma or renal cell carcinoma. PLoS One 2014;9:e90353.

35. Pietra G, Manzini C, Rivara S, Vitale M, Cantoni C, Petretto A, et al. Melanoma cells inhibit natural killer cell function by modulating the expression of activating receptors and cytolytic activity. Cancer Res 2012;72:1407–15.

36. McGilvray RW, Eagle RA, Watson NF, Al-Attar A, Ball G, Jafferji I, et al. NKG2D ligand expression in human colorectal cancer reveals associations with prognosis and evidence for immunoediting. Clin Cancer Res 2009;15:6993–7002.

37. Carlsten M, Baumann BC, Simonsson M, Jadersten M, Forsblom AM, Hammarstedt C, et al. Reduced DNAM-1 expression on bone marrow NK cells associated with impaired killing of CD34+ blasts in myelodysplastic syndrome. Leukemia 2010;24:1607–16.

38. Carlsten M, Norell H, Bryceson YT, Poschke I, Schedvins K, Ljunggren HG, et al. Primary human tumor cells expressing CD155 impair tumor targeting by down-regulating DNAM-1 on NK cells. J Immunol 2009;183:4921–30.

39. Koo KC, Shim DH, Yang CM, Lee SB, Kim SM, Shin TY, et al. Reduction of the CD16(-)CD56bright NK cell subset precedes NK cell dysfunction in prostate cancer. PLoS One 2013;8:e78049.

40. Horton NC, Mathew PA. NKp44 and natural cytotoxicity receptors as damage-associated molecular pattern recognition receptors. Front Immunol 2015;6:31.

41. Wu JD, Higgins LM, Steinle A, Cosman D, Haugk K, Plymate SR. Prevalent expression of the immunostimulatory MHC class I chain-related molecule is counteracted by shedding in prostate cancer. J Clin Invest 2004;114:560–8.

42. Liu G, Lu S, Wang X, Page ST, Higano CS, Plymate SR, et al. Perturbation of NK cell peripheral homeostasis accelerates prostate carcinoma metastasis. J Clin Invest 2013;123:4410–22.

43. Crane CA, Austgen K, Haberthur K, Hofmann C, Moyes KW, Avanesyan L, et al. Immune evasion mediated by tumor-derived lactate dehydrogenase induction of NKG2D ligands on myeloid cells in glioblastoma patients. Proc Natl Acad Sci U S A 2014;111:12823–8.

44. Pasero C, Gravis G, Granjeaud S, Guerin M, Thomassin-Piana J, Rocchi P, et al. Highly effective NK cells are associated with good prognosis in patients with metastatic prostate cancer. Oncotarget 2015;6:14360–73.

45. Fong L, Carroll P, Weinberg V, Chan S, Lewis J, Corman J, et al. Activated lymphocyte recruitment into the tumor microenvironment following preoperative sipuleucel-T for localized prostate cancer. J Natl Cancer Inst 2014;106.doi:10.1093/jnci/dju268.

46. Miller AM, Lundberg K, Ozenci V, Banham AH, Hellstrom M, Egevad L, et al. CD4+CD25high T cells are enriched in the tumor and peripheral blood of prostate cancer patients. J Immunol 2006;177: 7398–405.

47. Sfanos KS, Bruno TC, Maris CH, Xu L, Thoburn CJ, DeMarzo AM, et al. Phenotypic analysis of prostate-infiltrating lymphocytes reveals TH17 and Treg skewing. Clin Cancer Res 2008;14:3254–61.

48. Anderson MJ, Shafer-Weaver K, Greenberg NM, Hurwitz AA. Tolerization of tumor-specific T cells despite efficient initial priming in a primary murine model of prostate cancer. J Immunol 2007;178: 1268–76.

49. Shafer-Weaver KA, Anderson MJ, Stagliano K, Malyguine A, Greenberg NM, Hurwitz AA. Cutting edge: tumor-specific CD8+ T cells infiltrating prostatic tumors are induced to become suppressor cells. J Immunol 2009; 183:4848–52.

Cancer Research

AAC-R American Association for Cancer Research

Inherent and Tumor-Driven Immune Tolerance in the Prostate Microenvironment Impairs Natural Killer Cell Antitumor Activity

Christine Pasero, Gwenaëlle Gravis, Mathilde Guerin, et al.

Updated version	Access the most recent version of this article at: doi:10.1158/0008-5472.CAN-15-1965

Cited articles	This article cites 48 articles, 22 of which you can access for free at: http://cancerres.aacrjournals.org/content/76/8/2153.full#ref-list-1

E-mail alerts	Sign up to receive free email-alerts related to this article or journal.
Reprints and Subscriptions	To order reprints of this article or to subscribe to the journal, contact the AACR Publications Department at pubs@aacr.org.
Permissions	To request permission to re-use all or part of this article, contact the AACR Publications Department at permissions@aacr.org.